Supporting Information:

Production, Collection, and Purification of ^{47}Ca for the Generation of ^{47}Sc through Isotope Harvesting at the National Superconducting Cyclotron Laboratory

E. Paige Abel[1,2], Katharina Domnanich[1,2], Hannah K. Clause[1,2], Colton Kalman[2], Wes Walker[2], Jennifer A. Shusterman[3,4], John Greene[5], Matthew Gott[5], Gregory W. Severin[1,2]*

[1]Department of Chemistry, Michigan State University, East Lansing, MI, 48824, USA

[2]National Superconducting Cyclotron Laboratory, Michigan State University, East Lansing, MI, 48824, USA

[3]Department of Chemistry, Hunter College of the City University of New York, New York, NY, 10065, USA

[4]Ph. D. Program in Chemistry, The Graduate Center of the City of New York, New York, NY, 10016, USA

[5]Physics Division, Argonne National Laboratory, Lemont, IL, 60439, USA

Introduction

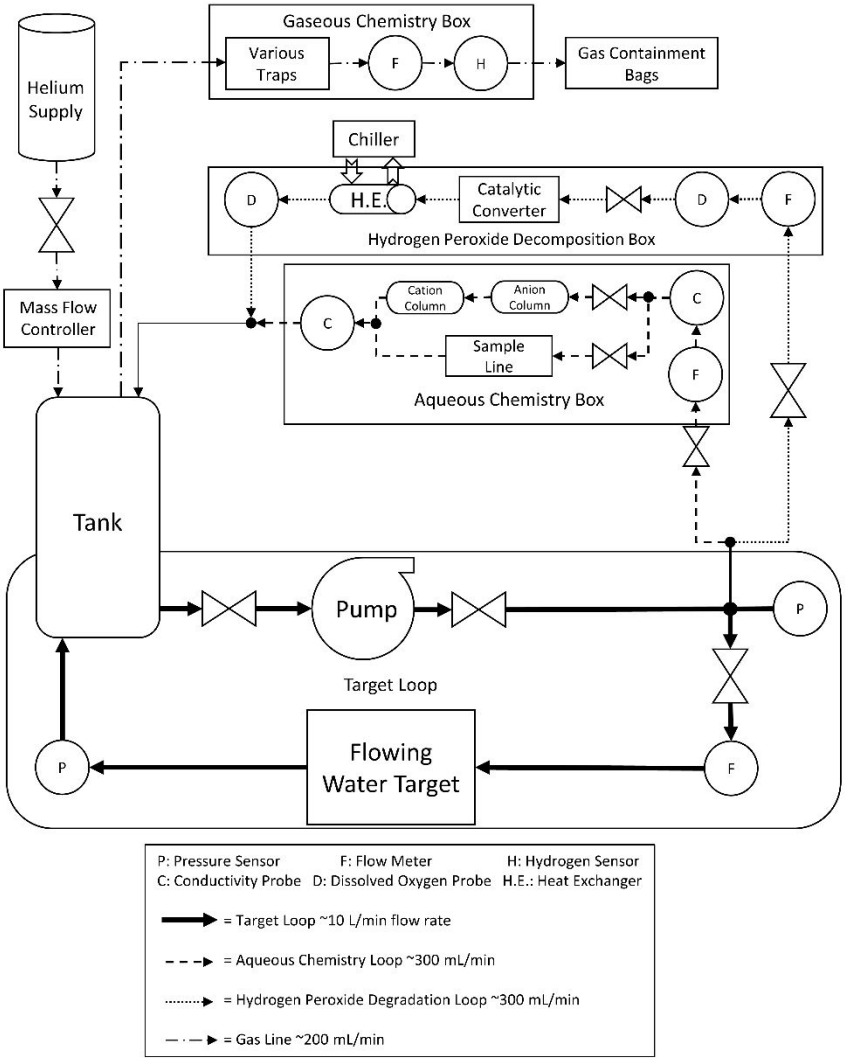

Figure S1: Schematic of the Isotope Harvesting System[1]
The solid outlines designate the different main subsystems: target loop, aqueous chemistry box, hydrogen peroxide decomposition box, and gas chemistry box. The solid circles the intersection of more than two lines indicate a T-connection and the double triangles with points facing each other indicate manual valves.

[1]Reprinted from Nuclear Instruments and Methods in Physics Research B, 478, E. Paige Abel, Katharina Domnanich, Colton Kalman, Wes Walker, Jonathan W. Engle, Todd E. Barnhart, Greg Severin, *Durability test of a flowing-water target for isotope harvesting*, 34-45, Copyright (2020), with permission from Elsevier. https://doi.org/10.1016/j.nimb.2020.05.011

Materials and Methods

Materials:

Though non-standard sample geometries were used for gamma spectrometry, no correction factors or additional errors were considered in quantifying radionuclides. Measurements have been performed that demonstrate about 10% difference in the quantification of these nuclides between a point source and a water sample and <10% for that between a point source and ions adsorbed on a resin bed. Absolute quantification based on the water samples was only performed for small activities to determine the total activity and production rate found for ^{47}Ca, where the 20% error in the branching ratios far outweighs the uncertainty from the geometry. When quantification was performed for radionuclides on the cation exchange resin beds, separation columns, or small volumes in falcon tubes at 25 cm from the detector face, no additional uncertainty for the geometry was used as it is a small correction. These measurements taken for the separation methods were also used to calculate the percent activity eluted so the absolute quantification was not necessary.

^{48}Ca Irradiation:

Calibrating Target Beam Current Readings

An unsuppressed current reading was measured on the target; this reading was proportional but not equivalent to the true current from the accelerated beam due to secondary electrons produced at the target by the ion beam. A calibrated faraday cup was used to measure the ion beam intensity at the lower and higher beam current settings used in this experiment. The measurements on the faraday cup were used to calibrate the concurrent unsuppressed readings on the target. Figure S2 shows the linear relationship between the unsuppressed target current readings and the calibrated readings from the faraday cup. This relationship was used to scale the beam current readings on the target measured on average every second throughout the experiment.

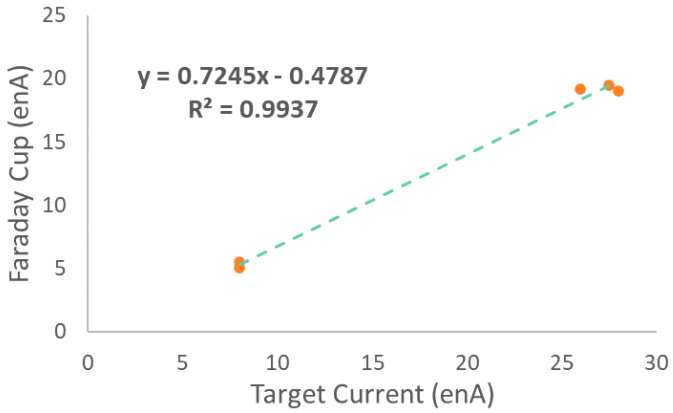

Figure S2: Calibration of Target Current Readings
The current recorded on a calibrated faraday cup and the unsuppressed target are given in electrical nanoamps (enA).

Production of ^{47}Ca:

The total produced ^{47}Ca activity and the recorded beam intensity throughout the irradiation were used to find the production rate, P, in terms of particles produced per incoming beam particle with Equation S1:

$$N_P = \sum_{i=1}^{n} [P \times I(t_i) \times (1 - e^{-\lambda \Delta t_i}) \times e^{-\lambda t_d}] \quad \text{(S1)}$$

where N_P is the number of produced nuclei, $I(t_i)$ is the beam current during the *i*th irradiation interval from t_i to t_{i+1}, λ is the decay constant of the produced radionuclide, and t_d is the time between the *i*th irradiation interval and the end of the irradiation. This segmented production equation accounts for fluctuations in beam intensity during the irradiation.

Collection and Sample Processing:

The nuclear data used to quantify the radionuclides collected on cation exchange resins 1-3 used in the harvesting system are given in Table S1. For the characteristic gamma-rays of ^{28}Mg, no uncertainty for the branching ratio was reported so an uncertainty of 10% was assumed.

Table S1: Nuclear Data Used to Quantify Radionuclides Collected on Cation Exchange Resins 1-3[1-10]

Radionuclide	Half-life	Gamma-Ray Energy (keV)	Branching Ratio (%)
^{24}Na	14.997 h	1368.6	99.9936(15)
^{27}Mg	9.458 m	843.8	70.94(9)
^{28}Mg	20.915 h	400.6	36(4)
		941.7	36(4)
		1342.2	54(5)
^{42}K	12.355 h	1524.6	18.08(9)
^{43}K	22.3 h	372.8	86.8(2)
		396.9	11.85(8)
		593.4	11.26(8)
		617.5	79.2(6)
^{44}K	22.13 m	368.2	2.3(4)
		651.4	3.0(5)
		726.5	3.8(6)
		1024.7	7(1)
		1126.1	8(1)
		1157.0	58(9)
		1499.5	8(1)
		1752.6	4.1(6)
^{45}K	17.18 m	174.28	74(5)
		1705.6	53(3)
^{47}Ca	4.536(3) d	489.2	5.9(12)
		807.9	5.9(12)
		1297.1	67(13)
^{44m}Sc	58.61 h	271.2	86.7(3)
^{47}Sc	3.3492 d	159.4	68.3(4)
^{48}Sc	43.67 h	983.4	100.1(5)
		1037.5	97.6(7)
		1312.1	100.1(7)

Purification of ^{47}Ca:

Recovery Yield and Radionuclidic Purity

Since the yield and radionuclidic purity of the ^{47}Ca processed with each of the separation methods was quite high (*i.e.*, 100% yield and radiopurity), the limit of detection for radionuclides that would influence these values was also found. For the yield, the limit of detection for ^{47}Ca was found for gamma spectra of the fraction taken just before ^{47}Ca was observed in the eluate, any fractions taken after ^{47}Ca was no longer observed in the eluate, and the column after all fractions were taken for a separation. These were the samples that were most likely to contain ^{47}Ca that was at or below the limit of detection. The largest influence on the radiopurity was any activity below the limit of detection for ^{43}K, since this was the radionuclide of the highest activity that eluted close to ^{47}Ca. Tailing elution behavior from this radionuclide could have occurred through the ^{47}Ca elution peak, affecting the radionuclidic purity. Therefore, the limit of detection of ^{43}K was found in each fraction that was considered for the total yield of ^{47}Ca.

In determining the limit of detection, only the highest intensity gamma-ray energy was considered for each radionuclide (*i.e.*, 1297 keV for ^{47}Ca and 372 for ^{43}K). The limit of detection was taken as the error in the counts over a range of 3.5 keV for ^{43}K and 5 keV for ^{47}Ca centered at their most intense characteristic gamma-ray. The total limit of detection for each of these values was the sum of the limit in each spectrum considered. The limit was then converted to a percentage in terms of the total ^{47}Ca activity (*i.e.*, the sum of eluted ^{47}Ca activity in each separation). This limit of detection was smaller than the error associated with the separation yield and the radionuclidic purity in all cases.

Stable Element Analysis:

Samples of 200 mL from water sample 1-4 were evaporated on a rotary evaporator and reconstituted in 10 mL of 1.4% HNO_3 each. The round bottom flasks used for the evaporation were first rinsed with 1.4% HNO_3 and then with MilliQ water twice. Additionally, all the purified ^{47}Ca samples from the three separation methods were combined and a sample was diluted by half for analysis, resulting in a solution of about 1.5 M HCl. Each of these samples was analyzed with a semi-quantitative method on inductively coupled plasma-optical emission spectroscopy to identify stable ions above the limit of detection of the instrument. The semi-quantitative method contains preset calibration information for 69 elements with a one-point calibration at 5 ppm from the following calibration check standards: Rare Earths, Precious Metals, Tellurium, Alkaline Earth Non-Transition Elements, and Fluoride Soluble Group. The samples were run with a blank check solution of 1.4% HNO_3 for the concentrated water samples and 1.5 M HCl for the combined, purified ^{47}Ca fractions. These blank samples served to help set the baseline for stable ions from the acid content of the samples and for the blank readings from the semi-quantitative method. Readings from the sample above the “blank” reading were further considered as described below.

Results and Discussion

Production of ^{47}Ca:

Distribution of ^{47}Ca Activity

The activity for each water sample withdrawn from the system and ion exchange resin used to collect activity from the system are given in Table S2. A total activity in the water remaining in the system following collection on cation exchange resin 5 is estimated by scaling the activity measured in water sample 5 to account for the larger volume of water in the whole system. The activity in water samples 1-4, cation exchange resins 1-5, the anion exchange resin, and the remaining water in the system give a total of 3.7(7) MBq of activity.

Table S2: ^{47}Ca Activity Measured in Each Water Sample and Cation Exchange Resin Bed

Sample	Activity (kBq)	Sample	Activity (kBq)
Water sample 1	7(1)	Cation Resin 1	3.0(6) X 10^2
Water sample 2	16(3)	Cation Resin 2	9(2) X 10^2
Water sample 3	25(5)	Cation Resin 3	1.2(2) X 10^3
Water sample 4	34(7)	Cation Resin 4	2.3(5) X 10^2
Water sample 5	42(8)	Cation Resin 5	3.1(6) X 10^2
Remaining water	7(1) X 10^2	Anion Resin	5(2)

LISE++ Support for Production Estimate at FRIB

The program LISE++ was used to verify the relative production rate of ^{47}Ca through fragmentation reactions with a 140 and a 189 MeV/nucleon ^{48}Ca. To find these values, the following settings where used in the program. The components in the beam line were (in order) a 0.57 mm thick target of Ti64 alloy (86% Ti, 10% Al, and 4% V by stoichiometry, 4.43 g/cm^3), a stripper layer of water (67% H, 33% O by stoichiometry, 1 g/cm^3), and a material layer of iron. This set up represents the isotope harvesting target as a thin shell of Ti64 alloy and a thick internal layer of water. As the beam travels through the water layer, ^{47}Ca is formed through fragmentation reactions on ^{1}H and ^{16}O/^{18}O nuclei. The product continues with a forward momentum and must reach the material layer to be "detected" by the program. Therefore, the thickness of the water layer was optimized for each beam energy, as it needs to be thick enough to allow for the beam to complete all possible fragmentation reactions and thin enough to allow for the products to have enough energy to escape and implant in the material layer. The water layer was optimized to 14.5 mm and 25.6 mm for the 140 and 189 MeV/nucleon beam, respectively. Using these settings, which are realistic for isotope harvesting and comparable to each other, the values in Table S3 were found.

Comparing the primary beam conversion to ^{47}Ca, the production rate with a 189 MeV/nucleon beam is predicted to be 170% of that with a 140 MeV/nucleon beam. This verifies that the production rate measured in this experiment with a 140 MeV/nucleon beam is an underestimation of the production rate expected at FRIB.

Table S3: ^{47}Ca Production with an 80 pnA ^{48}Ca Beam at 140 and 189 MeV/nucleon

Beam Energy (MeV/nucleon)	^{47}Ca production rate (pps)	^{48}Ca primary beam transmission rate (pps)	Percent primary beam conversion to ^{47}Ca
140	4.10×10^{9}	4.14×10^{11}	1.0
189	6.24×10^{9}	3.62×10^{11}	1.7

Purification of ^{47}Ca

Details about the fraction volume, liquid phase composition, and percent elution for each radionuclide are given in Table S4-S6 for a representative replicate of Separation methods 1-3, respectively. The uncertainty given for the recovery percent is from counting uncertainties; large errors result from low count rates and therefore, larger associated percent uncertainties. At the bottom of each table, two additional values are given for each radionuclide: the percentage that remained on the column after the last fraction was collected and the total percent that was eluted from the column. Any cell in the table that is blank indicates a value of zero.

Table S4: Example Replicate with Separation Method 1: DGA with 3 M HNO_3/3M HCl

Liquid Phase	Fraction Number	Fraction Volume (mL)	Volume Sum (mL)	Recovery Percent (%)							
				^{24}Na	^{28}Mg	^{42}K	^{43}K	^{47}Ca	^{44m}Sc	^{47}Sc	^{48}Sc
3 M HNO_3	1	15	15	100(5)	100(12)	100(9)	100(2)				
	2	7	22								
3 M HCl	3	10	32					3.4(5)			
	4	10	42					97(3)			
			Column						100(17)	100(3)	100(7)
			Total	100(5)	100(12)	100(9)	100(2)	101(3)			

Table S5: Example Replicate with Separation Method 2: AG MP-50 with HCl Gradient

Liquid Phase	Fraction Number	Fraction Volume (mL)	Volume Sum (mL)	Recovery Percent (%)							
				^{24}Na	^{28}Mg	^{43}K	^{47}Ca	^{44m}Sc	^{46}Sc	^{47}Sc	^{48}Sc
0.1 M HCl	1	20	20								
	2	10	30								
2 M HCl	3	5	35	100(19)	100(32)						
	4	4.5	39.5								

	5	4.5	44			34(2)					
	6	2	46			40(2)					
	7	2	48			19(1)					
	8	3	51			6.3(7)					
	9	2	53								
5 M HCl	10	2.1	55.1				15.8(7)				
	11	5	01.1				82(2)				
	12	2.4	62.5				1.7(3)				
			Column					100(5)	100(13)	100(1)	100(3)
			Total	100(19)	100(32)	100(3)	100(2)				

Table S6: Example Replicate with Separation Method 3: AG MP-50 with HCl/Methanol Gradient

Liquid Phase	Fraction Number	Fraction Volume (mL)	Volume Sum (mL)	Recovery Percent (%)							
				^{24}Na	^{28}Mg	^{43}K	^{47}Ca	^{44m}Sc	^{46}Sc	^{47}Sc	^{48}Sc
0.5 M HCl/90% MeOH	1	13	13								
	2	6	19								
	3	10	29								
	4	8	37								
2 M HCl/60% MeOH	5	14	51	6(3)	53(19)						
	6	16	67	57(10)	47(15)						
	7	13	80	37(9)							
	8	6	86								
2 M HCl/30% MeOH	9	7.5	93.5			7.5(5)					
	10	4.5	98			19(1)					
	11	3	101			23(1)					
	12	3	104			25(1)					
	13	4	108			17(1)					
	14	4.5	112.5			10(1)					
	15	4	116.5			1.6(5)					
	16	3.5	120								
4 M HCl	17	13	133				99(4)				
	18	7	140				1.6(4)				
			Column					100(27)	100(28)	100(2)	100(13)
			Total	100(14)	100(24)	103(3)	100(4)				

Stable Elemental Analysis:

The elements detected with the semi-quantitative ICP-OES method at a concentration of 0.05 ppm or higher in any of the samples are shown in Table S7. The concentrations listed for the combined, purified ^{47}Ca sample are corrected for the dilution made before analysis and are dissolved in approximately 150

mL of 3-5 M HCl. The elements detected in the concentrated water sample are only reported for water sample 3 since this sample was the last withdrawn before cation exchange resins were put in the system. The values given for the water sample are given at the concentrated level and are extrapolated to an approximate mass that was present in the entire water volume of the system (35 ± 4 L) at the time water sample 3 was withdrawn.

Overall, low levels were detected for all stable ions identified. Given these low levels, only the semi-quantitative analysis was performed. This method gives concentrations that are trusted within a factor of two as it uses a preset calibration that is not updated by the user each time a set of samples are analyzed, providing a helpful but semi-quantitative understanding of the stable element levels.[11,12] The calcium level detected in the combined, purified ^{47}Ca sample should not disrupt the use of a ^{47}Ca/^{47}Sc generator in future experiments or radiolabeling with the resulting ^{47}Sc. The small amount of stable calcium will move through the generator with the radioactive ^{47}Ca, leaving the ^{47}Sc free of calcium. The levels of metals such as Zn, Fe, Ni, Cu, etc. that could follow ^{47}Sc through the generator and interfere with radiolabeling in future experiment are present at low levels in both the purified ^{47}Ca sample and the concentrated water sample. The total estimated masses of the elements detected in the water sample are low enough that, if collected on a single resin in future experiments, they should not interfere with any chemistry steps following collection (*i.e.*, removal from collection resin, purification of ^{47}Ca, generation of ^{47}Sc, and radiolabeling with ^{47}Sc).

Table S7: Stable Element Semi-Quantification

All values reported in this table are given to only one significant figure with unknown accuracy due to the semi-quantitative nature of the measurement. The measured concentrations for elements in the blank for each sample type was approximately zero (-0.03 to 0.03 ppm) except for those listed in the table and cesium, which read about -14 ppm for blanks and samples, indicating that the preset calibration was misaligned. A dash signifies that an elemental concentration was < 0.05 ppm for that sample. The "Total System Water" referred to in the rightmost column is the 35 L remaining in the system after water sample 3 was removed.

Element	Wavelength (nm)	Concentration (ppm)				Estimated Mass in Total System Water Based on Sample 3 (µg)
		Blank-1.5 M HCl	Combined Purified ^{47}Ca samples	Blank-1.4% HNO_3	Concentrated Water Sample #3	
Ca	396.847	-	2	-	0.1	200
Ca	422.673	-	3	-	0.2	400
Mg	279.553	-	0.2	-	0.08	200
Na	589.592	0.1	0.2	0.09	0.4	700
Si	251.611	0.7	0.2	-	0.09	400
B	249.772	0.06	-	-	0.3	200
Fe	238.204	-	0.1	-	0.05	80
Zn	213.857	-	0.3	-	0.3	100
Cu	327.395	-	-	-	0.05	80

References

(1) Firestone, R. B. Nuclear Data Sheets for A = 24. *Nucl. Data Sheets* **2007**, *108*, 2319–2392. https://doi.org/10.1006/ndsh.2001.0008.

(2) Shamsuzzoha Basunia, M. Nuclear Data Sheets for A = 27. *Nucl. Data Sheets* **2011**, *112* (8), 1875–1948. https://doi.org/10.1016/j.nds.2011.08.001.

(3) Basunia, M. S. Nuclear Data Sheets for A = 28. *Nucl. Data Sheets* **2013**, *114* (10), 1189–1291. https://doi.org/10.1016/j.nds.2015.11.003.

(4) Singh, B.; Cameron, J. A. Nuclear Data Sheets for A = 42. *Nucl. Data Sheets* **2001**, *92* (1), 1–145. https://doi.org/10.1006/ndsh.2001.0001.

(5) Singh, B.; Chen, J. Nuclear Data Sheets for A = 43. *Nucl. Data Sheets* **2015**, *126*, 1–150. https://doi.org/10.1016/S0090-3752(80)80029-9.

(6) Chen, J.; Singh, B.; Cameron, J. A. Nuclear Data Sheets for A = 44. *Nucl. Data Sheets* **2011**, *112*, 2357–2495. https://doi.org/10.1016/S0090-3752(80)80029-9.

(7) Burrows, T. W. Nuclear Data Sheets for A = 45. *Nucl. Data Sheets* **2008**, *109* (1), 171–296. https://doi.org/10.1016/j.nds.2007.12.002.

(8) Peker, L. K. Nuclear Data Sheets Update for A=46. *Nucl. Data Sheets* **1993**, *68*, 271–310.

(9) Burrows, T. W. Nuclear Data Sheets for A = 47. *Nucl. Data Sheets* **2007**, *108*, 923–1056. https://doi.org/10.1016/j.nds.2006.05.005.

(10) Burrows, T. W. Nuclear Data Sheets for A = 48. *Nucl. Data Sheets* **2006**, *107*, 1747–1922. https://doi.org/10.1016/j.nds.2006.05.005.

(11) Neubauer, K.; Thompson, L. Semiquantitative Analysis in ICP-OES and ICP-MS. *Spectroscopy*. 2011, pp 24–31.

(12) Chen, H.; Dabek-zlotorzynska, E.; Rasmussen, P. E.; Hassan, N.; Lanouette, M. Evaluation of Semiquantitative Analysis Mode in ICP-MS. *Talanta* **2008**, *74*, 1547–1555. https://doi.org/10.1016/j.talanta.2007.09.037.